Calculation of correlation functions of hard spheres in the generalized mean spherical approximation

B. B. Deo and A. C. Naik
Department of Physics, Utkal University, Bhubaneswar 751004, Orissa, India
(Received 3 May 1982; revised manuscript received 4 November 1982)

Wiener-Hopf factorization technique as suggested by Baxter has been used to solve the Ornstein-Zernike equation for a system of hard spheres in the framework of a generalized mean spherical model. The method reported here yields unambiguous and accurate values of the radial distribution function $g(r)$, direct correlation function $C(r)$, and the structure function $S(k)$. These thermodynamic quantities have been calculated from low to fairly high densities and, with a normalized $g(R)$, they have been compared with the molecular-dynamics values of Alder and Hecht.

I. INTRODUCTION

The experimentally determined structure function curves for simple monatomic liquids like argon, sodium, or potassium look astonishingly similar to those calculated for an assembly of hard spheres.[1] So it is natural to consider a statistical system of hard spheres as a practical unperturbed first reference system for dense fluids.[2–4] Based on this observation, Andersen, Chandler, and Weeks[5] have suggested a simple phenomenological equation for the radial distribution function,

$$g(r)=g_0(r)e^{-\xi(r)/k_BT}, \tag{1}$$

where $\xi(r)$ is a renormalized potential and $g_0(r)$ is the hard-sphere radial distribution function. The simple Eq. (1) has been tested for several real fluids. It is in exceedingly good agreement with all available data. Obviously enough, the small discrepancies have been attributed by the above authors to be mainly due to the nonavailability of reliable hard-core values $g_0(r)$. One of the major aims of the present work is to suggest a novel method for obtaining accurate values for $g_0(r)$ as well as other correlation functions for the hard-sphere system.

It has to be realized that for dense fluid the determination of the $g_0(r)$ from its basic definition involving the partition function is extremely difficult. Therefore the study of the integral equations for $g_0(r)$ provides a better alternative and is highly instructive. There are two such well-known equations, one by Born and Green[6] (BG) and the other by Ornstein and Zernike[7] (OZ), with various closures. The BG equation has the advantage that it predicts a possible phase transition for a system of hard spheres at $\rho R^3=0.95$, where R is the hard-sphere diameter and ρ is the particle number density. But it breaks down at high density. Therefore in this paper, we shall confine ourselves to the simpler and more elegant OZ equation, which relates the direct correlation function $C(r)$ to the total correlation function $h(r)$ $[h(r)=g(r)-1]$ by

$$h(r)=C(r)+\rho\int C(\vec{r}')h(|\vec{r}-\vec{r}'|)d\vec{r}'. \tag{2}$$

The closure is made by proposing $C(r)$ as

$$C(r)=g(r)(1-e^{v(r)/k_BT}), \tag{3}$$

called the Percus-Yevick[8] (PY) equation, or

$$C(r)=h(r)-\ln g(r)-v(r)/k_BT, \tag{4}$$

called the hypernetted-chain[9] (HNC) equation. Out of the two closures the PY[10,11] equation is simpler and perhaps more accurate, and using this, the OZ equation can be exactly solved for hard sphere. But the disadvantage of the PY approximation is that the equations of state obtained from virial and compressibility equations are not unique. Thus the value of correlation functions will be different. Since this will be the major point of our subsequent analysis, we further explain this point. The expression for pressure[6] is

$$\frac{p}{k_BT}=\rho-\tfrac{2}{3}\pi\rho^2\int_0^\infty \frac{dv(r)}{dr}g(r)r^3dr \tag{5}$$

and leads to the virial equation[6] of state for the hard spheres

$$\frac{p(v)}{\rho k_BT}=(1+\eta+\eta^2-3\eta^3)/(1-\eta)^3, \tag{6}$$

whereas another expression can be deduced from the compressibility[6] relation

$$\frac{1}{k_BT}\frac{\partial p}{\partial\rho}=\left[1+\rho\int h(r)d^3r\right]^{-1}. \tag{7}$$

By integrating, the pressure p^c is now given by

$$\frac{p^{(c)}}{\rho k_B T}=(1+\eta+\eta^2)/(1-\eta)^3 . \quad (8)$$

It is called the compressibility equation of state. For low densities $\eta\to 0$ both Eqs. (6) and (8) are identical, but for $\eta\to 1$, i.e., for dense fluids, one is quite different from the other. The two expressions for pressure come from the same radial distribution function. But they differ because the latter is not exact. From Eq. (5), for a hard core,

$$\frac{p}{\rho k_B T}=1+4\eta g(R_+) \quad (9)$$

(R_+ and R_- are defined as $R+0$ and $R-0$, respectively). The two values of $g(R_+)$ so obtained will be denoted by $g^v(R_+)$ and $g^c(R_+)$ of which $g^c(R_+)$ is found to be closer to the exact value calculated by computer experiment.

We shall show that the theory can be made consistent by postulating the appropriate discontinuity in $C(r)$ at $r=R$. That there exists a jump for $C(r)$ across R has already been shown by Croxton.[12] He considered a restricted class of diagrams, called a small watermelon class, and obtained an expression which shows a striking jump of $C(R)$ from R_+ to R_-. But that does not remove the inconsistencies altogether. So we follow a different technique, which is outlined in Secs. II and III.

The Fourier transform of the OZ equation is

$$\tilde{h}(k)=\tilde{C}(k)+\rho\tilde{C}(k)\tilde{h}(k) . \quad (10)$$

To solve this, a function $\tilde{A}(k)$ is introduced such that

$$\tilde{A}(k)=1-\rho\tilde{C}(k)=[1+\rho\tilde{h}(k)]^{-1} . \quad (11)$$

A Wiener-Hopf[13] factorization is carried out and

$$\tilde{A}(k)=\tilde{Q}(k)\tilde{Q}(-k) . \quad (12)$$

The function $\tilde{Q}(k)$ is regular, has zeros in the lower half plane, and can be written in the form

$$\tilde{Q}(k)=1-2\pi\rho\int_0^R dr\, e^{ikr}Q(r) . \quad (13)$$

$Q(r)$ is a real function and is very useful for the following discussions.

For the PY approximation $C(r)$ is strictly zero beyond the hard-core diameter R. In this case one calculates $g^v(R)$. To arrive at the correct value of $g(R)$, Waisman, Lebowitz, and Percus[14–17] have followed a mean spherical model in which $C(r)$ is extended. We have followed the treatment which represents a generalized mean spherical model where $Q(r)$ is extended rather than $C(r)$. This has got certain advantage in the sense that knowledge of $Q(r)$ not only gives $C(r)$ beyond $r>R$, but the whole thermodynamics also becomes clear via the inverse compressibility equation. $Q(r)$ and its Fourier transform $\tilde{Q}(k)$ have to satisfy certain boundary conditions and analytic properties, respectively. So in the simplest case it is chosen as a polynomial beyond $r>R$. It is extended until $r=R+\sigma$. Then σ is made smaller and smaller to the extent that the calculated values of $g(r)$ become independent of σ. This extrapolates to the correct value of $g^c(R_+)$ as obtained from the compressibility equation of state. It should be noted that

$$g(R_+)-g(R_-)=C(R_+)-C(R_-)$$

is a direct consequence of the OZ equation. The value of $C(r)$ for $r<R$ is unaffected when the range is extended beyond R to $R+\sigma$.

Further, the values of the structure function $S^v(k)$ reported in literature refer to the Fourier transform of $h^v(r)$ which would follow from less accurate $g^v(r)$. We shall report the values of $S^c(k)$ obtained by Fourier transforming $g^c(r)$. We also report $C(r)$ in Sec. III for several densities.

It must be emphasized at this stage that none of the values of $g^c(r)$ and $g^v(r)$ agree with the molecular-dynamics (MD) data of Alder and Hecht.[18] These data will be tabulated under $g^{\mathrm{MD}}(r)$. It is possible to obtain this $g^{\mathrm{MD}}(R)$ by choosing a different adjusted value for $Q'(R_+)$. The values of $g^{\mathrm{EQ}}(r)$ calculated in this phenomenological way agree quite well with the MD data. The corresponding $S(k)$ values have also been calculated. These are reported in Sec. IV.

II. FORMALISM

The Wiener-Hopf and Baxter[13] formalism has been extensively discussed in the literature.[1] So a brief outline is given here with more emphasis on our method of computation of $g_0(r)$.

With the help of Eqs. (11) and (12) it can be shown that Eq. (2) can be split into

$$rC(r)=-Q'(r)+2\pi\rho\int_r^R dt\, Q'(t)Q(t-r) \quad (14)$$

for $0<r<R$ and if $C(r)=0$ for $r>R$, and

$$rh(r)=-Q'(r)+2\pi\rho\int_0^R dt(r-t)h(|r-t|)Q(t) \quad (15)$$

for $r>0$, where $Q'(r)$ is the derivative of $Q(r)$.

Since $h(r)=-1$ for $r<R$,

$$Q'(r)=ar+b \quad \text{for } 0<r<R . \quad (16)$$

By integrating and comparing, one gets

$$Q(r)=a/2(r^2-R^2)+b(r-R) , \quad (17)$$

where

$$a=(1+2\eta)/(1-\eta)^2 , \tag{18}$$

$$b=-\tfrac{3}{2}R\eta/(1-\eta)^2 , \tag{19}$$

and

$$\eta=\pi R^3\rho/6 . \tag{20}$$

It is easily seen that

$$C(r)=-a^2+6\eta[(1+\eta/2)^2/(1-\eta)^4]r/R - \eta/2[a^2(r/R)^3] \tag{21}$$

for $r<R$.

Once $Q(r)$, $h(r)$, and $C(r)$ are known in the range $0<r<R$, the value of $h(r)$ for $r>R$ can be obtained through the Fourier transform of

$$\tilde{h}(k)=\{[\tilde{Q}(k)\tilde{Q}(-k)]^{-1}-1\}/\rho . \tag{22}$$

But the inverse transform $h(r)$ from $\tilde{h}(k)$ poses some computational difficulty and is found not to converge rapidly. However, this can be computed fairly accurately by Wertheim's zone by zone method. Alternatively, Baxter[13] has suggested to work with the one-sided Fourier transform of $h(r)$, that is,

$$\tilde{h}_+(k)=-\left[\int_0^R dr\, e^{ikr}\left[Q'(r)+2\pi\rho\int_0^{R-r} dt\, th(t)Q(t+r)\right]\right]\Big/\tilde{Q}(k) . \tag{23}$$

The inverse transform of $\tilde{h}_+(k)$ leads to $h(r)$ relatively easily for hard core alone. However, this relation is not particularly suitable if $C(r)$ or $Q'(r)$ exists beyond the hard core. We find an infinity-subtraction method works very well for this problem. The high-k behavior of $\tilde{h}(k)$, denoted by $\tilde{h}_\infty(k)$, is subtracted. The inverse transform of

$$\Delta\tilde{h}(k)=\tilde{h}(k)-\tilde{h}_\infty(k)$$

is calculated rather than $\tilde{h}(k)$ itself. For the hard core $\tilde{h}_\infty(k)$ is taken to be

$$\tilde{h}_\infty(k)=C_\infty\cos(kR)/k^2-S_\infty\sin(kR)/k^3 , \tag{24}$$

where the coefficients are

$$C_\infty=2R(a+b/R) \tag{25}$$

and

$$S_\infty=2a-4\pi\rho R\left[\frac{a}{2}R^2+bR\right](a+b/R) . \tag{26}$$

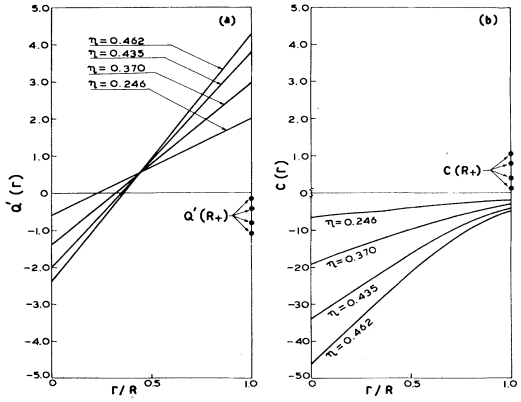

FIG. 1. (a) $Q'(r)$ at four different densities. Dots at the bottom represent the $Q'(R_+)$ values. Lowest value of $Q'(R_+)$ refers to the highest η. (b) $C(r)$ at four different densities. Dots at the top refer to the $C(R_+)$ values. Highest value of $C(R_+)$ refers to the highest η.

The $h_\infty(r)$ is easily calculated exactly from the integral tables

$$h_\infty(r)=S_\infty/2 \quad \text{for} \quad r<R , \qquad h_\infty(r)=(S_\infty-C_\infty)/2r \quad \text{for} \quad r\geq R . \tag{27}$$

The $h_\infty(r)$ is to be added to the Fourier transform of $\Delta\tilde{h}(k)$. It is to be noted and we emphasize that only in this way have we been able to strictly obtain $h(r)$ close to -1 for $r<R$, which must be satisfied in all computations.

The radial distribution function $g_0(r)$ obtained by this inversion is $g^v(R_+)$ at $r=R_+$, appropriate to the more inaccurate virial equation of state. This is the $g(r)$ normally used in all calculations using hard-core results. The structure function $S^v(k)$ calculated using Eq. (22) would also give theoretically less-accurate values.

As suggested earlier, to get the correct value of $g^c(R_+)$, one has to introduce the discontinuity in $Q'(r)$ and $C(r)$. We shall discuss these points in Sec. III.

III. CALCULATION OF CORRELATION FUNCTIONS IN THE GENERALIZED MEAN SPHERICAL MODEL

Assuming that $Q(r)$ and $C(r)$ exist beyond the hard core until, for example, $R+\sigma$, the Baxter equation (15) becomes

TABLE I. $Q'(R_+)$ for $g^v(R)$, $g^c(R)$, and $g^{MD}(R)$ for different densities. η is packing fraction.

η	$g^v(R)$	$g^c(R)$	$g^{MD}(R)$
0.246	0	−0.11	−0.10
0.370	0	−0.41	−0.32
0.435	0	−0.79	−0.55
0.462	0	−1.04	−0.69

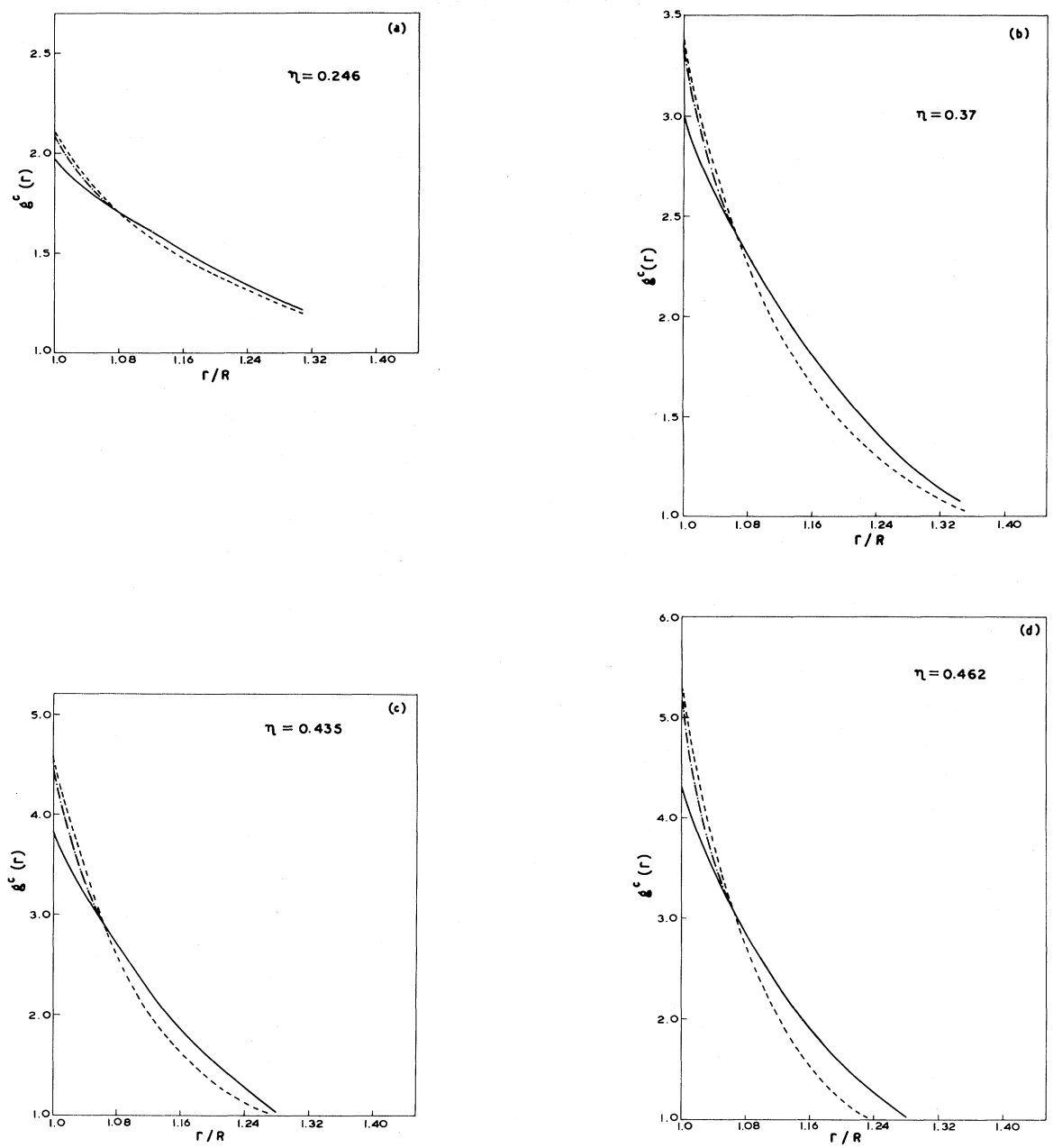

FIG. 2. (a) $g^c(r)$ values for $\eta=0.246$ with the dashed line for $\sigma=0.9$, the dot-dashed line for $\sigma=0.1$, and the solid line for $\sigma=0$. (b) Same as (a) for $\eta=0.37$. (c) Same as (a) for $\eta=0.435$. (d) Same as (a) for $\eta=0.462$.

$$Q'(r)=-rh(r)+2\pi\rho\int_0^{R+\sigma}dt(r-t)h(|r-t|)Q(t)\ . \tag{28}$$

For $r<R$ this reduces to

$$Q'(r)=Ar+B+2\pi\rho\int_R^{R+\sigma}dt(r-t)g(|r-t|)Q(t)\ . \tag{29}$$

Here

$$A=1-2\pi\rho\int_0^R Q(t)dt-2\pi\rho\int_R^{R+\sigma}Q(t)dt \tag{30}$$

and

$$B=2\pi\rho\int_0^R tQ(t)dt+2\pi\rho\int_R^{R+\sigma}tQ(t)dt\ . \tag{31}$$

One can see that the last term in Eq. (29) does not vanish in the region for small r, $0<r<\sigma$. So $Q'(r)$

TABLE II. Calculated values of $g^c(r)$ compared with corresponding $g^{MD}(r)$ values for four different densities at $\sigma=0.1$ and $R=1$.

r/R \ η	0.246		0.370		0.435		0.462	
	$g^{MD}(r)$	$g^c(r)$	$g^{MD}(r)$	$g^c(r)$	$g^{MD}(r)$	$g^c(r)$	$g^{MD}(r)$	$g^c(r)$
1.00	2.07	2.081	3.30	3.396	4.36	4.600	4.95	5.300
1.02		1.910		3.000		3.800		4.140
1.04	1.92	1.849	2.77	2.634	3.44	3.220	3.73	3.528
1.06		1.780		2.470		2.940		3.100
1.08	1.78	1.747	2.36	2.312	2.68	2.687	2.89	2.859
1.12	1.65	1.626	2.03	2.044	2.17	2.265	2.23	2.349
1.16	1.53	1.527	1.76	1.801	1.79	1.891	1.76	1.903
1.20	1.43	1.436	1.55	1.588	1.49	1.579	1.44	1.539
1.24	1.35	1.353	1.37	1.406	1.27	1.323	1.20	1.249
1.28	1.28	1.279	1.23	1.252	1.10	1.119	1.01	1.025
1.32	1.21	1.212	1.10	1.124	0.97	0.960	0.89	0.858
1.36	1.16	1.153	1.01	1.019	0.87	0.841	0.80	0.739
1.40	1.10	1.100	0.94	0.936	0.80	0.755	0.73	0.660
1.44	1.06	1.055	0.88	0.871	0.74	0.699	0.69	0.615
1.48	1.02	1.017	0.84	0.824	0.70	0.667	0.66	0.597
1.52	0.99	0.984	0.81	0.792	0.69	0.656	0.65	0.601
1.56	0.97	0.958	0.78	0.774	0.69	0.662	0.65	0.623
1.60	0.95	0.937	0.79	0.767	0.69	0.681	0.67	0.658
1.64	0.94	0.921	0.79	0.770	0.71	0.711	0.69	0.703
1.68	0.92	0.911	0.80	0.783	0.75	0.750	0.74	0.756
1.72	0.92	0.905	0.82	0.803	0.80	0.796	0.80	0.815
1.76	0.92	0.904	0.85	0.829	0.86	0.848	0.87	0.877
1.80	0.92	0.907	0.88	0.862	0.91	0.903	0.96	0.942
1.84	0.92	0.914	0.91	0.899	0.98	0.962	1.03	1.008
1.88	0.93	0.925	0.96	0.941	1.04	1.023	1.10	1.076
1.92	0.95	0.939	1.00	0.987	1.09	1.086	1.17	1.145
1.96	0.97	0.957	1.06	1.036	1.15	1.151	1.22	1.214
2.00	0.99	0.978	1.10	1.087	1.22	1.217	1.28	1.284
2.04	1.00	0.998	1.14	1.127	1.27	1.257	1.31	1.319
2.08			1.15	1.145	1.26	1.255	1.28	1.300
2.12			1.14	1.145	1.22	1.224	1.23	1.246
2.16			1.13	1.133	1.17	1.176	1.16	1.175
2.20			1.10	1.113	1.12	1.121	1.10	1.098
2.24			1.08	1.089	1.06	1.065	1.03	1.025
2.28			1.06	1.063	1.01	1.013	0.99	0.962
2.32			1.04	1.037	0.98	0.967	0.95	0.910
2.36			1.02	1.012	0.96	0.931	0.91	0.873
2.40			1.00	0.991	0.94	0.904	0.88	0.850
2.44			0.98	0.973	0.92	0.887	0.87	0.841
2.48			0.97	0.959	0.91	0.880	0.87	0.843
2.52			0.96	0.949	0.92	0.881	0.87	0.856
2.56			0.96	0.943	0.92	0.890	0.89	0.876
2.60			0.95	0.944	0.92	0.904		
2.64			0.96	0.944				

for $r<R$ is not necessarily linear in r. However, expanding $g(r)$ near $r\simeq R$ to the lowest order in σ, the last term in Eq. (29) becomes

$$2\pi\rho\int_R^{R+\sigma} dt\,(r-t) \times[g(R)+(R-t+r)g'(R-t+r)+\cdots]Q(t)\,.$$

Hence Eq. (29) will reduce to

$$Q'(r)=Ar+B+2\pi\rho g(R)\int_R^{R+\sigma} Q(t)dt\,(r-t)+\cdots\,, \tag{32}$$

which is linear. Furthermore, if one constructs the $Q(t)$'s beyond $t>R$ such that

$$\int_R^{R+\sigma} dt\,Q(t)=0 \tag{33}$$

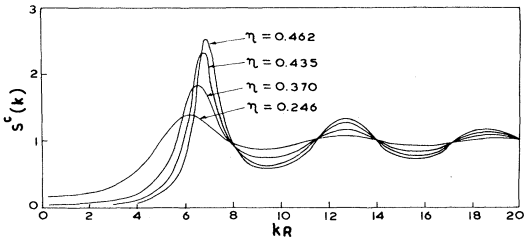

FIG. 3. $S^c(k)$ values for four different densities.

and

$$\int_R^{R+\sigma} dt\, tQ(t)=0\ ,$$

Eq. (32) reduces to a linear form.

$Q'(r)=ar+b$ for $r<R$ with a and b given by (18)—(20). Equation (33) forms two important constraints for $Q(r)$ beyond R.

Introducing a change of variable

$$z=2(r-R)/\sigma-1 \tag{34}$$

and using the conditions

$$Q_\infty(z)\,|_{z=-1}=Q(R_+)=0$$

and

$$Q_\infty(z)\,|_{z=+1}=Q(R+\sigma)=0\ , \tag{35}$$

we find that for $r>R$

$$Q_\infty(z)=-Q'\sigma(1-6z^2+5z^4)/16 +Q'\sigma(3z-10z^3+7z^5)/16\ , \tag{36}$$

TABLE III. Calculated values of structure function $S^c(k)$ at four different densities at $\sigma=0.1$.

kR \ η	0.246	0.370	0.435	0.462
1	0.1565	0.0561	0.0314	0.0242
2	0.1967	0.0711	0.0395	0.0303
3	0.2907	0.1079	0.0595	0.0454
4	0.5034	0.2042	0.1117	0.0845
5	0.9333	0.5103	0.2871	0.2151
6	1.3343	1.4646	1.1328	0.9018
7	1.2078	1.6269	2.1841	2.5745
8	0.9745	0.9801	1.0065	1.0287
9	0.8787	0.7606	0.6787	0.6369
10	0.9007	0.7749	0.6748	0.6243
11	0.9895	0.9353	0.8638	0.8184
12	1.0670	1.1347	1.1724	1.1824
13	1.0661	1.1634	1.2612	1.3208
14	1.0093	1.0311	1.0572	1.0744
15	0.9621	0.9216	0.8903	0.8743
16	0.9566	0.9022	0.8558	0.8306
17	0.9867	0.9610	0.9325	0.9148
18	1.0226	1.0452	1.0596	1.0653
19	1.0326	1.0764	1.1170	1.1406
20	1.0125	1.0321	1.0523	1.0647

TABLE IV. Calculated values of $C(r)$ at four different densities for $\sigma=0.1$ and $R=1$.

r/R \ η	0.246	0.37	0.435	0.462
0.00	−6.887	−19.219	−34.315	−46.345
0.10	−6.312	−17.243	−30.526	−41.073
0.20	−5.742	−15.289	−26.782	−35.866
0.30	−5.182	−13.378	−23.127	−30.789
0.40	−4.637	−11.531	−19.607	−25.907
0.50	−4.113	−9.769	−16.265	−21.285
0.60	−3.614	−8.113	−13.148	−16.987
0.70	−3.146	−6.586	−10.299	−13.079
0.80	−2.713	−5.208	−7.764	−9.625
0.90	−2.321	−4.000	−5.587	−6.691
1.00	−1.975	−2.985	−3.813	−4.341
1.00	0.105	0.410	0.786	1.080
1.01	−0.008	−0.031	−0.059	−0.081
1.02	−0.039	−0.154	−0.296	−0.406
1.03	−0.028	−0.110	−0.211	−0.289
1.04	−0.002	−0.009	−0.018	−0.024
1.05	0.018	0.073	0.140	0.192
1.06	0.025	0.099	0.190	0.260
1.07	0.016	0.062	0.120	0.135
1.08	−0.002	−0.009	−0.017	−0.024
1.09	−0.015	−0.058	−0.112	−0.155
1.10	0.000	0.000	0.000	0.000

where $Q'\sigma$ is the derivative of Q_∞ at $z=-1$, and as such, Eq. (36) satisfies all the constraints of Eq. (33). For $\sigma\to 0$, $Q'_\infty(R)=Q'(R_+)$.

The discontinuity as estimated for both $Q'(r)$ and $C(r)$ is shown in Fig. 1. The $Q'(R_+)$'s are the bottom bold points of Fig. 1(a) and the $C(R_+)$'s are the top bold points of Fig. 1(b).

The Fourier transform $\tilde{Q}(k)$ is of the form

$$\tilde{Q}(k)=\tilde{Q}_{hc}(k)+\tilde{Q}_\infty(k)\ , \tag{37}$$

where $\tilde{Q}_{hc}(k)$ is given by Eq. (13) and

$$\tilde{Q}_\infty(k)=-2\pi\rho\int_R^{R+\sigma} e^{ikr}Q(r)dr\ . \tag{38}$$

TABLE V. Calculated values of $C(r)$ at four different densities for $\sigma=0.5$ and $R=1$.

r/R \ η	0.246	0.370	0.435	0.462
1.00	0.105	0.410	0.786	1.080
1.05	−0.007	−0.029	−0.057	−0.078
1.10	−0.036	−0.143	−0.274	−0.377
1.15	−0.025	−0.098	−0.189	−0.259
1.20	−0.002	−0.008	−0.015	−0.021
1.25	0.015	0.061	0.118	0.162
1.30	0.020	0.080	0.154	0.212
1.35	0.012	0.49	0.092	0.130
1.40	−0.001	−0.007	−0.013	−0.018
1.45	−0.011	−0.044	−0.084	−0.116
1.50	0.000	0.000	0.000	0.000

TABLE VI. Calculated values of $C(r)$ at four different densities for $\sigma=0.9$ and $R=1$.

r/R \ η	0.246	0.370	0.435	0.462
1.00	0.105	0.410	0.786	1.080
1.09	−0.007	−0.028	−0.055	−0.075
1.18	−0.034	−0.133	−0.256	−0.351
1.27	−0.023	−0.089	−0.171	−0.235
1.36	−0.001	−0.007	−0.013	−0.019
1.45	0.013	0.053	0.101	0.139
1.54	0.017	0.068	0.130	0.179
1.63	0.010	0.041	0.078	0.108
1.72	−0.001	−0.005	−0.010	−0.015
1.81	−0.009	−0.035	−0.068	−0.093
1.90	0.000	0.000	0.000	0.000

Transforming the integral in Eq. (38) to the z space one gets

$$\tilde{Q}_\infty(k)=-2\pi\rho\sigma\, e^{ik(R+\sigma/2)}\int_0^1 e^{ik\sigma z/2}Q(z)dz\ , \tag{39}$$

which is more amenable to direct computation.

As before, we make an inverse transform of

$$\Delta\tilde{h}(k)=\tilde{h}(k)-\tilde{h}_\infty(k)\ .$$

$\tilde{h}_\infty(k)$ is again given by Eq. (24) with changed coefficients:

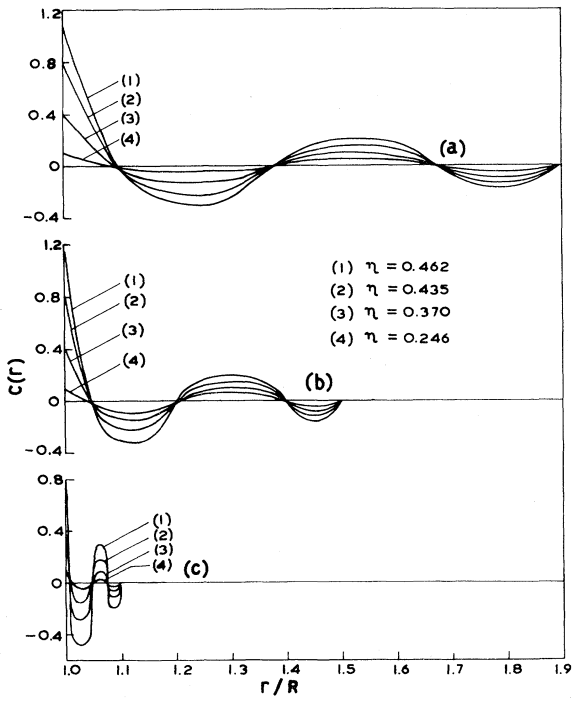

FIG. 4. $C(r)$ values beyond the hard-core radius. (a) $\sigma=0.9$, (b) $\sigma=0.5$, and (c) $\sigma=0.1$.

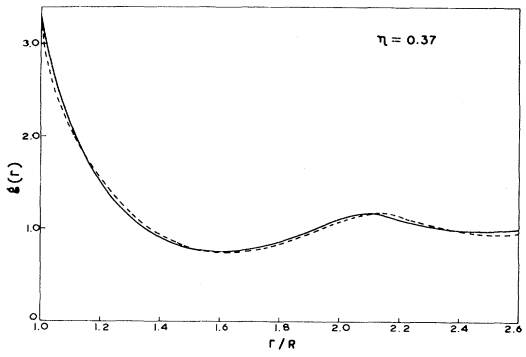

FIG. 5. $g^{MD}(r)$ values and $g^{EQ}(r)$ values are represented by the solid and dashed line, respectively, for $\eta=0.37$.

$$C_\infty=2R(a+b/R)-4RQ' \tag{40}$$

and

$$S_\infty=2a+[24Q'-12(a+b/R)]\eta/(1-\eta)+64Q'R/\sigma\ . \tag{41}$$

Using Eq. (39) in Eq. (37) and finally making use of Eq. (22) one can evaluate $S^c(k)$.

MD results for hard-sphere distribution functions by Alder and Hecht are available for four different densities. We now attempt to compute the $g^c(r)$ at these densities with the additional extension to $Q(r)$. Take, for instance, $\eta=0.246$. The $g^c(R_+)$ calculated for this density is 2.08. The $Q'(R_+)$ to obtain this $g^c(R_+)$ is -0.11. Using this $Q'(R_+)$, we recalculate $Q(r)$ and $g^c(r)$.

Similarly, we furnish the $Q'(R_+)$'s for $g^v(R)$, $g^c(R)$, and $g^{MD}(R)$ for four different densities in Table I. For each density $g^c(r)$ is calculated for different σ, of which $\sigma=0.05$, 0.1, and 0.9 are reported. At a particular density, $g^c(r)$ changes appreciably from $\sigma=0.9$ to 0.3 but there is almost no change in $g^c(r)$ for smaller values of σ, especially for $\sigma=0.1$ and 0.05. The values of $g^c(r)$ for various r up to $r/R=1.32$ are plotted in Fig. 2 for three different σ, such as $\sigma=0$, 0.1, and 0.9. The $g(r)$ for $\sigma=0$ relates to $g^v(r)$. There is a remarkable change in $g(r)$ for $\sigma=0$ and 0.1 in the region $r/R\simeq 1$ and almost no change when $r/R\gg 1$. The $g^c(r)$ values for $\sigma=0.1$ is closer to MD data. So $g^c(r)$ for $\sigma=0.1$ are compared with the MD data at four different densities in Table II.

The structure function $S^c(k)$ is computed at four different densities and plotted in Fig. 3. The values are furnished in Table III. The results do not show much changes over the $S^v(k)$ in the low-k region.

Even more striking is the behavior of the direct correlation function with σ. With $Q(z)$ known, $C(r)$ can be easily obtained from Eq. (14). One gets

TABLE VII. Calculated values of $g^{EQ}(r)$ compared with $g^{MD}(r)$ at four different densities for $\sigma=0.1$ and $R=1$.

r/R \ η	0.246		0.37		0.435		0.462	
	$g^{MD}(r)$	$g^{EQ}(r)$	$g^{MD}(r)$	$g^{EQ}(r)$	$g^{ML}(r)$	$g^{EQ}(r)$	$g^{MD}(r)$	$g^{EQ}(r)$
1.00	2.07	2.070	3.30	3.301	4.36	4.360	4.95	4.950
1.04	1.92	1.849	2.77	2.635	3.44	3.226	3.73	3.530
1.08	1.78	1.747	2.36	2.315	2.68	2.690	2.89	2.866
1.12	1.65	1.627	2.03	2.045	2.17	2.271	2.23	2.356
1.16	1.53	1.527	1.76	1.801	1.79	1.894	1.76	1.903
1.20	1.43	1.436	1.55	1.589	1.49	1.581	1.44	1.552
1.24	1.35	1.353	1.37	1.406	1.27	1.321	1.20	1.247
1.28	1.28	1.279	1.23	1.252	1.10	1.119	1.01	1.024
1.32	1.21	1.212	1.10	1.124	0.97	0.960	0.89	0.857
1.36	1.16	1.153	1.01	1.019	0.87	0.841	0.80	0.738
1.40	1.10	1.101	0.94	0.936	0.80	0.755	0.73	0.654
1.44	1.06	1.055	0.88	0.871	0.74	0.699	0.69	0.615
1.48	1.02	1.016	0.84	0.824	0.70	0.668	0.66	0.598
1.52	0.99	0.984	0.81	0.792	0.69	0.656	0.65	0.602
1.56	0.97	0.958	0.78	0.774	0.69	0.662	0.65	0.623
1.60	0.95	0.937	0.79	0.767	0.69	0.681	0.67	0.659
1.64	0.94	0.921	0.79	0.770	0.71	0.712	0.69	0.704
1.68	0.92	0.911	0.80	0.783	0.75	0.751	0.74	0.756
1.72	0.92	0.905	0.82	0.803	0.80	0.798	0.80	0.817
1.76	0.92	0.904	0.85	0.829	0.86	0.847	0.87	0.877
1.80	0.92	0.907	0.88	0.862	0.91	0.905	0.96	0.942
1.84	0.92	0.914	0.91	0.899	0.98	0.962	1.03	1.008
1.88	0.93	0.925	0.96	0.941	1.04	1.023	1.10	1.076
1.92	0.95	0.939	1.00	0.987	1.09	1.086	1.17	1.145
1.96	0.97	0.957	1.06	1.036	1.15	1.151	1.22	1.214
2.00	0.99	0.978	1.10	1.087	1.22	1.217	1.28	1.284
2.04	1.00	0.998	1.14	1.127	1.27	1.257	1.31	1.319
2.08			1.15	1.145	1.26	1.255	1.28	1.299
2.12			1.14	1.145	1.22	1.224	1.23	1.246
2.16			1.13	1.133	1.17	1.176	1.16	1.175
2.20			1.10	1.113	1.12	1.121	1.10	1.098
2.24			1.08	1.089	1.06	1.065	1.03	1.025
2.28			1.06	1.063	1.01	1.012	0.99	0.962
2.32			1.04	1.037	0.98	0.967	0.95	0.910
2.36			1.02	1.012	0.96	0.930	0.91	0.873
2.40			1.00	0.991	0.94	0.904	0.88	0.850
2.44			1.98	0.973	0.92	0.887	0.87	0.841
2.48			0.97	0.959	0.91	0.881	0.87	0.843
2.52			0.96	0.949	0.92	0.881	0.87	0.856
2.56			0.96	0.943	0.92	0.890	0.89	0.876
2.60			0.95	0.942	0.92	0.903		
2.64			0.96	0.943				

$$rC(r)=-Q'(r)+2\pi\rho\int_r^R Q'(t)Q(t-r)dt+2\pi\rho\left[[Q(t-r)Q_\infty(t)]_R^{R+\sigma}-\int_R^{R+\sigma}\frac{d}{dt}[Q(t-r)]Q_\infty(t)dt\right]. \tag{42}$$

For $R>r$, $C(r)$ is the same as that obtained by Baxter, Wertheim,[10] and Thele.[11] But when $R+\sigma>r>R$, it follows from Eq. (42) that

$$rC(r)=-Q'_\infty(r)\,. \tag{43}$$

This direct correlation function has been calculated for four different densities with varying σ. The values of $C(r)$ are given in Tables IV–VI for $\sigma=0.1$, 0.5, and 0.9. The results are plotted in Fig. 4. The hypothesized $C(r)$ now shows a peak at

$r/R=1$, falling to zero after two oscillations. As σ is decreased, the amplitudes of the small peaks increase and ultimately shrink to the axis.

IV. CALCULATION OF $g^{EQ}(r)$

It is to be noted at this stage that $g^c(r)$ and $g^v(r)$ agree with MD data when $r \gg R$ but differ near $r \simeq R$. However it is possible to obtain $g^{MD}(R)$ by choosing the exact value of $Q'(R_+)$ as shown in the third column of Table I. This changed $Q'(R_+)$ also improves the other $g(r)$ values which we designate as $g^{EQ}(r)$, and the agreement with MD data is better. The comparative results of correlation functions are reported in Table VII for all the four densities, but Fig. 5 is drawn only for $\eta=0.37$. The $S(k)$ are also calculated and are found not to be very much different from $S^c(k)$.

The merit of the technique will be further revealed when one attempts to include attractive potentials along with the hard core. In that case, one need not use the elaborate procedure of Smith,[19] Tosi[20] *et al.*, and Hoye and Blum.[21,22] One has to assume the existence of $Q(r)$ beyond the hard core and with proper discontinuity of $Q'(r)$ fit $g(r)$ to the MD data for the said potential. Once $Q(r)$ is known for the entire range, the thermodynamics becomes transparent. The work along these lines is being pursued.

ACKNOWLEDGMENTS

One of the authors (A.C.N.) gratefully acknowledges the University Grants Commission, India, for the award of a fellowship. The computational help of the Computer Centre, Utkal University, is acknowledged.

[1]J. A. Barker and D. Henderson, Rev. Mod. Phys. 48, 587 (1976).
[2]J. L. Lebowitz and E. M. Waisman, Phys. Today 33, 24 (1980).
[3]F. Lado, Mol. Phys. 31, 1117 (1976).
[4]Y. Rosenfeld and N. W. Aschroft, Phys. Rev. A 20, 1208 (1979).
[5]H. C. Anderson, D. Chandler, and J. D. Weeks, Adv. Chem. Phys. 34, 105 (1976).
[6]P. A. Egelstaff, *An Introduction to the Liquid State* (Academic, New York, 1975).
[7]L. S. Ornstein and F. Zernike, Z. Phys. 27, 761 (1926).
[8]J. K. Percus and G. J. Yevick, Phys. Rev. 110, 1 (1958).
[9]T. Morita and K. Hiroike, Prog. Theor. Phys. 23, 1003 (1960).
[10]M. S. Wertheim, Phys. Rev. Lett. 10, 321 (1963).
[11]E. Thele, J. Chem. Phys. 39, 474 (1963).
[12]C. A. Croxton, J. Phys. C 7, 3723 (1974).
[13]R. J. Baxter, Aust. J. Phys. 21, 563 (1968).
[14]J. L. Lebowitz and J. K. Percus, Phys. Rev. 144, 251 (1966).
[15]E. Waisman and J. L. Lebowitz, J. Chem. Phys. 52, 4307 (1970).
[16]E. Waisman and J. L. Lebowitz, J. Chem. Phys. 56, 3086 (1972).
[17]E. Waisman and J. L. Lebowitz, J. Chem. Phys. 56, 3093 (1972).
[18]B. J. Alder and C. E. Hecht, J. Chem. Phys. 50, 2032 (1968).
[19]E. R. Smith, Mol. Phys. 38, 823 (1979).
[20]D. K. Chaturbedi, G. Senatre, and M. P. Tosi, International Centre for Theoretical Physics Report No. IC/80/165 (unpublished).
[21]L. Blum and J. S. Hoye, J. Stat. Phys. 16, 399 (1977).
[22]L. Blum and J. S. Hoye, J. Stat. Phys. 19, 317 (1978).